Catalysis Today 49 (1999) 363–375

NMR probe for heterogeneous catalysis with isolated reagent flow and magic-angle spinning

Paul K. Isbester[a], Andrew Zalusky[a], David H. Lewis[b], Michelle C. Douskey[a], Marie J. Pomije[a], Kent R. Mann[a], Eric J. Munson[a,*]

[a] *University of Minnesota, 207 Pleasant St. S.E., Minneapolis MN 55455, USA*
[b] *Varian Nuclear Magnetic Resonance Instruments, 2607 Midpoint Dr., Fort Collins CO 80525, USA*

Abstract

We have developed an isolated flow MAS NMR probe to enable simultaneous observation of events occurring on a catalytic surface with characterization of the effluent gas using an external analytical instrument. The probe design is unique in that it uses ceramic ball bearings to support the rotor. The spinning and spectroscopic capabilities of the probe were proven by obtaining a ^{13}C CP/MAS NMR spectrum of hexamethylbenzene at MAS rates of 2 kHz. The flow capabilities of the probe were demonstrated by observing methanol adsorption onto zeolite HZSM-5 and by studying conformational changes of a vapochromic sensor material when it was exposed to volatile organic compounds. The variable-temperature capabilities were shown by monitoring the change in the ^{207}Pb chemical shift of $Pb(NO_3)_2$ as a function of temperature. Temperatures >300°C were achieved for the probe. The reaction of methanol to dimethyl ether on zeolite HZSM-5 was used to demonstrate the ability of the probe to study heterogeneous catalysis reactions in situ. The observed products varied depending on whether flow vs. batch conditions were used. Under flow conditions only dimethyl ether was observed. In previous studies under sealed (i.e. batch) conditions, an equilibrium was observed between methanol and dimethyl ether. © 1999 Elsevier Science B.V. All rights reserved.

1. Introduction

NMR spectroscopy is an extremely powerful technique for the in situ investigation of reactions that occur on heterogeneous catalysts [1,2]. Since these methods have been reviewed extensively; only a brief introduction is presented here. In the past, there have been two approaches for performing in situ NMR studies of heterogeneous catalysis reactions. The first method used flow gases over a static catalyst bed [3–5]. The reaction products were collected for analysis using a gas chromatograph or GC/MS. This approach best simulates a typical industrial reactor in that it emulates a flow reactor system, including introduction of new reactants and collection of products, with the added benefit of in situ observation of the reactants/products on the catalyst bed. The main disadvantage of this approach is that the peaks in the NMR spectrum were broadened by chemical shift anisotropy (CSA), which for ^{13}C can result in linewidths of 200 ppm or more. For this reason most NMR studies of catalytic reactions were performed using sealed samples, in which magic-angle spinning (MAS) could be used to average chemical shift anisotropy and produce narrow lines [6–15]. In this approach, either a glass ampoule or ceramic rotor was filled with the catalyst and reactant and, subse-

---

*Corresponding author. Fax: +1-612-626-7541; e-mail: munson@chem.umn.edu

PII: S0920-5861(98)00450-7

quently, sealed. Two alternative methods were used to heat the sample. In the first, the ampoule/rotor was heated externally in an oven for a prescribed amount of time, cooled, and an NMR spectrum acquired of the reactants/products [6–8]. After the spectrum was acquired, the ampoule/rotor was reheated to observe further reactions on the catalyst or opened for analysis by GC/MS. In the second method, the ampoule/rotor was heated in the NMR spectrometer, permitting the direct observation of the reaction while it occurred in the NMR spectrometer [9–15]. The disadvantage of this approach is that the ampoule/rotor was sealed prior to analysis. This approach best emulates a batch reactor. The resulting product distribution may be very different from that observed in a flow reactor system, because it is convoluted by changing reactant-to-product ratios and potential reactant–product interactions.

The ideal solution to these problems would be to design a system that could combine both the gas flow (with subsequent analysis of products) with the high-resolution NMR capability produced by MAS. Some of the parameters of this ideal system are described below. The rotor containing the catalyst could be heated or cooled depending on the reaction to be studied and should have a temperature range of 173 to 723 K. The rotor should spin at the magic angle as fast as possible, but have a minimum spinning speed of >2 kHz to acquire high-resolution spectra. At higher temperatures, slower spinning speeds may be acceptable as increased molecular motion will result in narrower linewidths for most species. There should be perfect isolation between the product and reactor streams and any drive/bearing gas used for MAS. The pressure in the reactant/product gas streams should have a range from 0.1 to 10 atm. Satisfying all of these requirements is difficult, given that the current MAS technology in most commercial probes has an upper limit of $\leq$523 K, and none of them provide for flow combined with MAS.

Recently, there have been several new NMR probe designs that have attempted to address at least some of the requirements described in the previous paragraph [16–20]. The first report of a MAS NMR probe that allowed reactant gas to flow over a catalyst bed was by Hunger and Horvath [16]. This design used a commercial Bruker 7-mm MAS probe that was modified to incorporate an injection tube into the MAS rotor. The tube reached to the bottom of the rotor and gas flowed over a catalyst bed as it exited at the top of the rotor. With this design, they were able to heat samples to 423 K at ambient flow pressures and MAS rates of 3 kHz. The primary limitations of this design are the high temperature restrictions imposed by the use of a commercial NMR probe and the inability to collect product gases for future analysis. In a subsequent study, the authors devised a method to perform product analysis in their flow MAS reactor external to the NMR spectrometer [17]. The MAS rotor was encapsulated in a glass vessel designed to permit injection of reactant gas and to collect the product gases for analysis by GC. This approach allows the comparison of the results of a flow MAS experiment to a similar flow-reactor study. The disadvantage is that the two analyses are performed separately under conditions which are not identical. Goguen and Haw [18] developed a similar probe design based on a Chemagnetics Pencil probe. This design also incorporates an injection tube to permit gas to flow through a catalyst bed and exits through a hole in the drive tip of the rotor. The advantage of the Chemagnetics design is an increased temperature range (up to 523 K). Two recent designs have been proposed that rely on magic-angle hopping (MAH) to average chemical shift anisotropy rather than MAS [19,20]. The MAH experiment, first performed by Maciel and others [20,21], is a two-dimensional (2D) experiment in which the isotropic chemical shift is recorded in the first dimension, and the anisotropic chemical shift is detected in the second dimension. The rotation rate of the rotor can be very slow (a few Hz) which permits a closed reaction vessel to be maintained. The advantages of this design are derived primarily from the fact that the rotor is not required to spin rapidly, and in one of the designs, the rotor does not rotate a full 360° but reverses direction to return to its origin. Variable pressures can be used because gas-tight seals are utilized between the reaction vessel and the atmosphere. The friction created by these seals impede high-speed MAS but can be overcome by a mechanical MAH apparatus. Because the reaction vessel is sealed, quantitative analysis of the reaction products can be performed. Both isotropic and anisotropic chemical shift data are acquired, and in the isotropic dimension there are no spinning sidebands. The disadvantage of this design is that the data is acquired using a two-dimensional NMR experiment. This imposes several restrictions on the type of systems that can be studied. A major problem is that sensitivity is significantly reduced compared to a conventional one-dimensional experiment. This can be partially overcome by using a Carr–Purcell–Meiboom–Gill (CPMG) series of spin echoes to refocus the chemical shift for subsequent addition [22,23]. The system must remain stable during the entire 2D acquisition process to prevent artifacts from appearing in the spectrum. At high temperatures, linewidths for adsorbed species in catalysts such as zeolites are narrow, and a large number of t_1 increments may be required for optimum resolution. Despite the above limitations, the ability to maintain quantitative gas flow and to operate at variable pressures will continue to drive research on this design.

In this paper, we present a new design for performing flow MAS experiments that satisfies many of the foregoing requirements. One of the most difficult aspects of designing a flow MAS system using conventional MAS technology is that high-pressure bearing and drive gas, respectively, are required to support and propel the rotor. We have overcome this problem by developing a spinning system that utilizes ceramic ball bearings to support a spinning rotor. The use of ceramic bearings has several advantages compared to previous flow MAS designs, such as eliminating the need to have a bearing gas, improving gas-stream isolation by separating the drive and bearing regions of the rotor from the flow regions, and increasing the variable-temperature limits by keeping the drive and bearing regions close to ambient temperature. We show that several of the technical challenges for designing a flow MAS system have been overcome, including spinning a rotor with ceramic ball bearings, flowing the reactant/product gas stream through a spinning rotor and incorporating variable-temperature capabilities.

2. Experimental

2.1. Description of flow MAS module

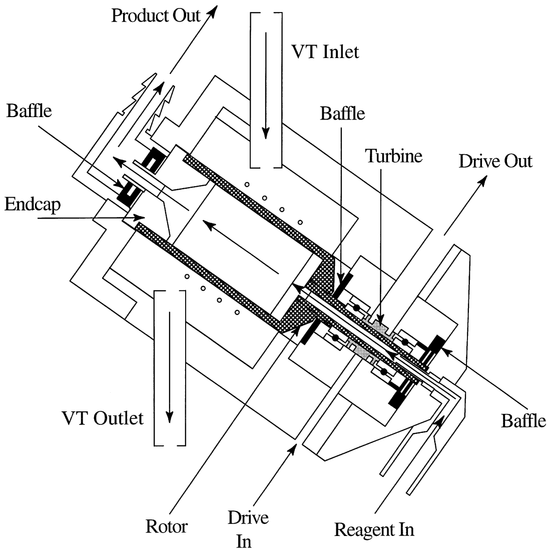

Fig. 1. Diagram of the flow VT MAS module.

The design of the flow MAS module is shown in Fig. 1. There are five main components in the module: body, cartridge, reactant gas endcap, product gas endcap, and rotor. An enlarged view of the cartridge is shown in Fig. 2, and an enlarged view of the product end of the rotor is shown in Fig. 3. The Vespel® module body has an o.d. of 1.500″ and a length of 2.35″ The Vespel® cartridge (o.d 0.750″, length 0.714″) is press-fitted into the body of the module. The cartridge supports two Si_3N_4 ball bearings (Miniature Precision Bearings, Keene, NH) and two sets of Vespel® baffles. The bearings have an o.d. of 0.3125″, an i.d. of 0.125″, and a width of 0.110″. The baffles are located at both ends of the cartridge, and are designed to isolate the drive gas from the reactant flow gas. The tolerance between the baffles and the rotor axle is ∼0.005″. Both of the bearings are housed in a single cartridge, because a previous design in which the bearings were located in two different pieces resulted in significant alignment problems. The rotor is supported exclusively by the two bearings. A turbine is press-fitted onto the rotor and is located inside the cartridge between the two bearings. The turbine has an o.d. of 0.235″ and has eight notches. On both sides of the turbine notches are rings designed to serve as baffles between the drive gas and the bearings. The tolerance between the rings and the cartridge is ∼0.005″. The turbine is powered by compressed gas, which is injected through a small hole (0.050″ diameter) that is tangential to the notches of the turbine. A larger slit (0.750″×0.150″) opposite from the small hole is the drive gas exit. An oil hole (0.125″ diameter) for each bearing is located between the

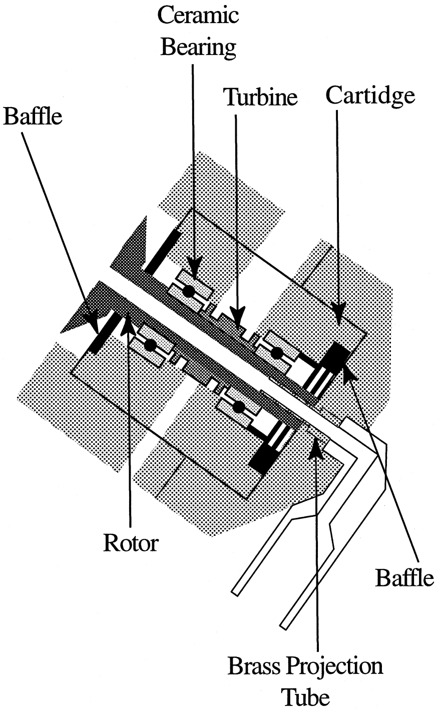

Fig. 2. Enlargement of the reactant/drive area of the flow VT MAS module.

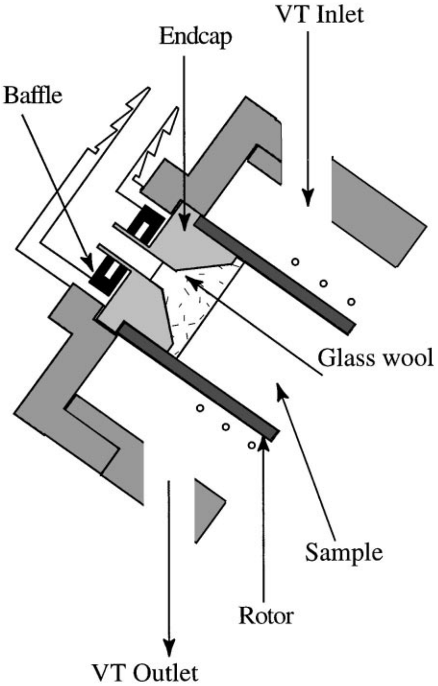

Fig. 3. Enlargement of the product collection area of the flow VT MAS module.

bearing and the baffles at the end of the cartridge. These holes permit the bearings to be oiled without removing them from the module and serve as additional vents for the drive gas. We used a light-weight synthetic hydrocarbon-based oil (Nye Lubricants, New Bedford, MA) and have never observed resonances in the NMR spectrum from the oil. We believe that the oil is not getting to the sample area of the module because of the aspirator effect from the high-pressure drive gas (vide infra), as the drive exhaust pulls the oil from the bearings and out of the module rather than pushing it into the sample chamber or into the reagent flow. We intend to analyze the product stream for oil using GC or GC/MS to prove this hypothesis. The combination of the baffles and vent holes provide excellent isolation between the drive gas and reactant gas, even at drive pressures as high as 80 psi.

The rotor is constructed from COMBAT® boron nitride, grade A (Carborundum, Amherst, NY). Boric oxide is used as a binder for the boron nitride, and will lose binding strength over time when exposed to moisture. The binder melts at 823 K, so the rotors are heated to 773 K for 18 h in a muffle furnace to dehydrate the rotors. After the heating cycle the rotors are more resistant to abrasions from bearings and baffles. The rotors are then stored in a desiccator and redried occasionally to remove adsorbed water. Unlike conventional MAS rotors, which are typically a hollow cylinder with plastic endcaps/drive tips, the flow MAS rotor is one piece of boron nitride with two distinct sections, the axle and the sample chamber. The axle section supports and propels the rotor. It has a 0.125″ o.d., 0.0625″ i.d., and is 0.755″ long. Reactant gas enters the axle end of the rotor through the smaller end of a brass projection tube (0.0625″ o.d., 0.050″ i.d., 0.175″ projecting into rotor). The larger end of the tube (o.d. 0.300″) is press-fitted in the reactant endcap. The projection tube forces the gas flow into the rotor. Typically, the i.d. of the rotor is the same size or slightly smaller than the o.d. of the brass projection tube. During the course of ‘breaking in’ a rotor, the boron nitride on the inside of the rotor is worn away by the brass projection tube until the rotor spins freely.

This process guarantees that the tolerance between the rotor and the projection tube is as close as possible. The reactant gas flows through the axis section into the sample chamber. The sample chamber section of the rotor has an o.d. of 0.551″, an i.d. of 0.394″, and is 1.05″ long. Glass wool is used to restrict the solid sample to the sample chamber region without restricting flowing gas. An endcap constructed of boron nitride is used to seal the rotor and direct the product gas into the product gas endcap. The endcap has a small projection (0.100″ o.d., 0.050″ i.d., and 0.150″ long) that extends from the rotor endcap into the product gas endcap. A series of baffles are located in the product gas endcap to isolate the sample region of the module body from the product gas stream. The tolerances at this end of the rotor are less restrictive (0.015″) to provide for the rotor wobbling.

Reactant gas is injected into the spinning module through the reactant module endcap. This endcap is press-fitted onto the cartridge and is held in place by four 1/56 screws threaded into the body of the module. Gas enters the reactant module endcap through a Kel-F elbow and directed through the brass projection tube into the rotor. Product gas exits the rotor through the product module endcap via an elbow. Variable-temperature gas enters through the top of the module and exits through the bottom. The inlet has been designed so that the gas passes through four small holes which direct it into the sample chamber without directly impinging on the rotor. This increases the maximum flow rate that can be used, minimizing temperature gradients and increasing the maximum temperature by reducing thermal stress on the heater element. The gas exits the spinning module and mixes with a large amount of purge and drive gases to cool the top of the probe. We have found this method to be effective for temperatures >300°C.

2.2. Configuration for flow-MAS experiments

The experimental setup for a typical flow-MAS experiment is shown in Fig. 4. Compressed N_2 gas is used as a carrier gas for the reactant/product gas stream and is controlled by a Brook Instrument 5850E mass-flow controller. The N_2 carrier gas could be directed either directly to the flow probe or through a bubbler containing the desired reagent (i.e. benzene, methanol, etc.) and into the flow-MAS probe. After the gases exit the flow-MAS probe, they are collected in a cold finger using dry ice/acetone to condense the products.

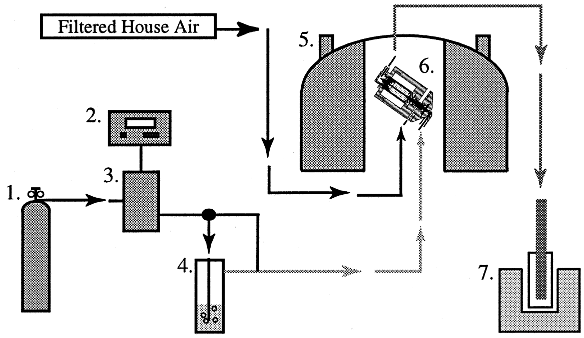

Fig. 4. Experimental setup used for flow-MAS NMR experiments. (1) Compressed N_2 gas; (2) mass-flow controller; (3) N_2 mass flow valve; (4) solvent bubbler; (5) magnet; (6) flow-MAS module; and (7) dry ice trap.

2.3. NMR spectroscopy

All ^{13}C NMR spectra were acquired using a Chemagnetics CMX-300 spectrometer operating at 75.4 MHz for ^{13}C. The flow-MAS module was mounted on a slightly modified Chemagnetics coaxial design probe that had additional holes for Teflon tubes containing the reactant and product gas streams. A standard Chemagnetics variable-temperature stack and controller was used to provide variable-temperature gas. All spectra were acquired with ^1H decoupling and using either single pulse (SP) excitation or cross polarization (CP). In view of the larger coil volume, typical decoupling powers were between 16 and 36 kHz. The spinning speed was monitored by attaching a shielded coaxial wire to the spinning module and observing the signal induced in the wire. The signal oscillated at a rate corresponding to the spinning frequency. We confirmed that the correct spinning rate was being measured by comparing it to the rotation frequency determined from spinning sidebands in a sample of hexamethylbenzene.

3. Results and discussion

We determined that there are three major technical challenges to designing an isolated flow VT MAS

NMR probe. The first challenge is to acquire an NMR spectrum of a rotor being spun using ceramic ball bearings. Prototypes of a ceramic ball bearing MAS module that could spin >5 kHz were developed in the early 1990's by Otsuka Electronics, but this technology was not pursued further. The second challenge is to design a system such that the reactant/product gas streams were isolated from the drive gas. The third challenge is to incorporate variable-temperature capabilities into the spinning module.

We demonstrated the ability to perform NMR spectroscopy by acquiring a ^{13}C CP/MAS NMR spectrum of hexamethylbenzene spinning at 1.75 kHz (spectrum not shown). Both the linewidth and sensitivity were comparable to that observed in our standard 7.5 mm Chemagnetics probe. This demonstrates the ability to obtain high-resolution solid-state NMR spectra at reasonable spinning speeds using ceramic ball bearings.

The isolation of the product/reactant gas streams was then investigated. A flow meter was used to monitor the flow rate of gases from the reactant (inlet) and product (exit) ends of the rotor. At slow spinning speeds (<1 kHz) with an empty or loosely packed rotor, there was excellent isolation at both the product and reactant ends of the rotor. At higher spinning speeds, there was a slight inward flow (<1 ml/min) on the reactant end as a result of negative pressure. We suspect that the high-pressure drive gas is acting like an aspirator and creating a slight vacuum. In the future, we will design a longer projection tube that will hopefully minimize this problem. At the product end there is a considerable inward flow. We suspect that the spinning rotor is creating a vacuum at the product end, similar to the drive gas acting as an aspirator. In variable-temperature experiments, we can compensate for this because the variable-temperature gas is at a high enough pressure to create a positive flow out of the product end. While we believe that this is not a satisfactory solution to the problem (i.e. improving isolation at the product end would be better), we can at least ensure that the product gas is exiting through the product stream. We also flowed gas into the reactant end of the rotor at a rate of 300 ml/min, and observed that the gas rate emerging from the product end was consistent with that flow rate. We used a bubbler to measure flow rates at the product end, in which a soap bubble rose through a graduated cylinder and the flow rate was determined by the amount of time it took for the bubble to traverse a fixed volume. This method is semiquantitative at best, which limited our ability to accurately determine the product flow rates.

Our next goal was to demonstrate that the flow gas would be adsorbed onto a highly porous catalyst such as a zeolite. A rotor was loosely packed with non-activated zeolite HZSM-5 and spun at a rate of 1.8 kHz. High-purity N_2 gas, flowing at a rate of 200 ml/min, was used as the reactant/product gas stream; this stream was either used directly or passed through a bubbler containing 5 ml of unlabeled methanol. ^{13}C MAS NMR spectra were acquired every 2 min to monitor the adsorption of methanol on the catalyst. Fig. 5(a) shows the relative intensity of the

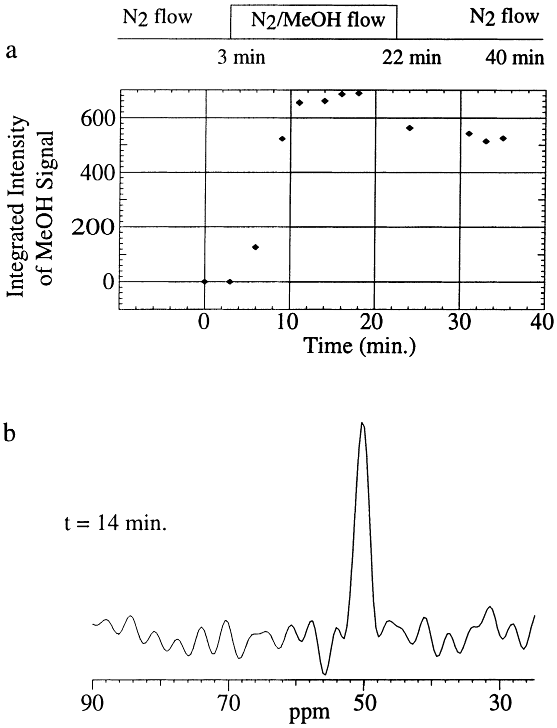

Fig. 5. (a) Plot of integrated peak intensity vs. time for methanol adsorption on HZSM-5 with MAS at 1.7 kHz and continuous N_2/methanol flow at 200 ml/min. Methanol bubbler was engaged during the indicated region from t=3 min through t=22 min. (b) Single pulse ^{13}C MAS NMR spectrum with proton decoupling of adsorbed methanol on HZSM-5 at t=14 min with 128 transients and 1.5 s pulse delay.

methanol signal as methanol vapor flowed through the rotor. A typical spectrum is shown in Fig. 5(b). At t=0 min, the nitrogen gas stream was passing only through the rotor. At t=3 min, the N_2 gas stream was directed through the bubbler. The intensity of the methanol signal rose sharply for the first 6–8 min, and then reached a plateau, probably indicating saturation of the HZSM-5 with methanol. At t=22 min, the N_2 gas stream was directed to bypass the methanol in order to purge the system. The signal intensity decreased slightly, probably due to nonadsorbed or loosely bound methanol emerging in the product stream.

The previous experiment demonstrated that gases would interact with highly porous catalysts, but it did not provide any information about the percentage of catalyst interacting with the adsorbate. In order to probe how much material was interacting with the gas stream, we studied a vapochromic sensor material, Pt[CN]Pt[$CNC_6H_4C_{10}H_{21}$] which undergoes a conformational change when it is exposed to volatile organic compounds (VOC) such as benzene and hexane [24]. Fig. 6 shows the aliphatic region of the ^{13}C CP/MAS NMR spectra of Pt[CN]Pt[$CNC_6H_4C_{10}H_{21}$] before and after exposure to benzene. The change in conformation upon exposure to benzene is evident in the spectra of this compound. Fig. 7 shows the aliphatic region of the ^{13}C CP/MAS NMR spectra of Pt[CN]Pt[$CNC_6H_4C_{10}H_{21}$] as N_2 gas saturated with benzene flowed through the material. The system was purged for 10 min with N_2 flow at 200 ml/min. At t=0 min, the N_2 gas stream was directed through a bubbler containing 5 ml of benzene. After 10 min, over 50% of the Pt[CN]Pt[$CNC_6H_4C_{10}H_{21}$] was converted to the exposed form, and after 30 min the spectrum showed that all of the Pt[CN]Pt[$CNC_6H_4C_{10}H_{21}$] was exposed to benzene. We also performed experiments with hexane, which interacts with this material more quickly than benzene. Fig. 8 shows the aliphatic region of the ^{13}C CP/MAS NMR spectra of Pt[CN]Pt[$CNC_6H_4C_{10}H_{21}$] as N_2 gas (150 ml/min) saturated with hexane flowed through the material. As was the case with benzene, the spectra changed with the addition of hexane. The difficulty in using hexane to study this system is twofold: one, the hexane resonances lie in the same region as the aliphatic

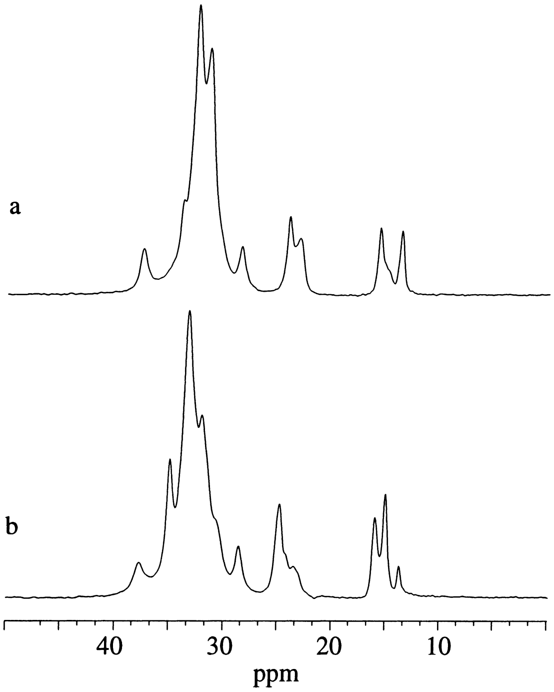

Fig. 6. ^{13}C CP/MAS NMR spectrum of Pt[CN]Pt[$CNC_6H_4C_{10}H_{21}$]. (a) Dry; and (b) exposed to benzene.

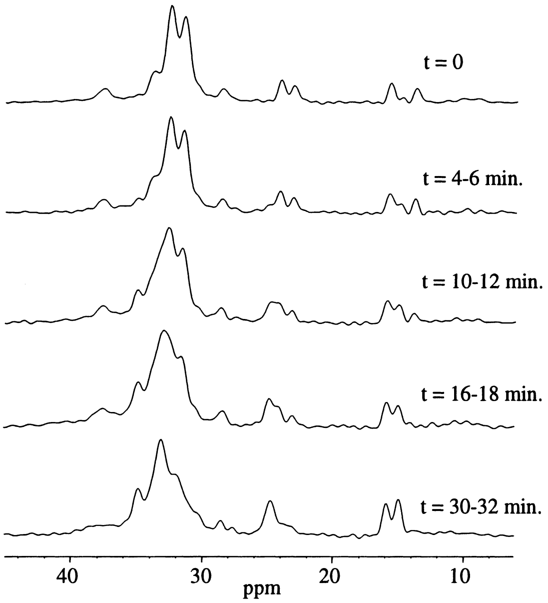

Fig. 7. ^{13}C flow CP/MAS NMR of Pt[CN]Pt[$CNC_6H_4C_{10}H_{21}$] at time increments t denoting time from start of continuous N_2/benzene flow at 200 ml/min. (1.7 kHz MAS, 25°C, 64 transients, 2.5 s pulse delay).

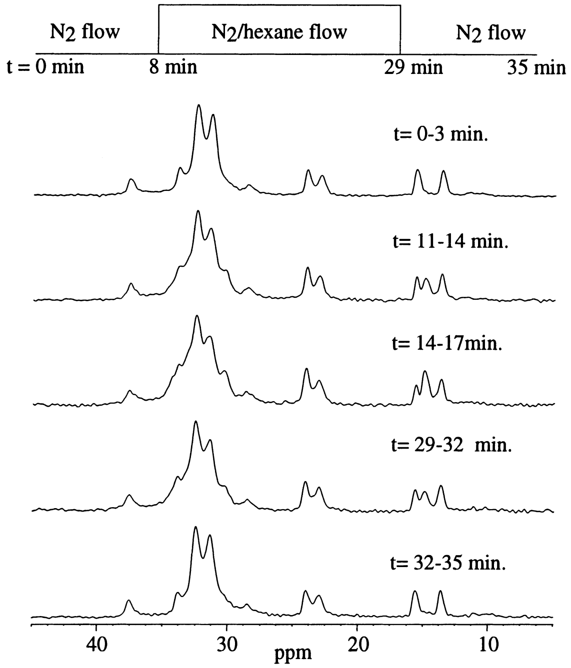

Fig. 8. ^{13}C flow CP/MAS NMR of $Pt[CN]Pt[CNC_6H_4C_{10}H_{21}]$ at time increments t with N_2 flow at 150 ml/min. The N_2 was directed through a bubbler containing 5 ml of hexane during the time denoted in the graph. (1.7 kHz MAS, 25°C, 64 transients, 2.5 s pulse delay).

portion of the $Pt[CN]Pt[CNC_6H_4C_{10}H_{21}]$, and two, the changes in the resonances of the $Pt[CN]Pt[CNC_6H_4C_{10}H_{21}]$ are not as dramatic as is the case for benzene. However, obvious changes can be seen in the spectrum, such as the broadening of the resonance at 38 ppm, and the changing line shapes of the peaks between 30 and 34 ppm. Neither of these changes overlap with the hexane resonances. After the N_2/hexane flow begins (t=8 min), the spectrum changes for the next 10 min. When the hexane is bypassed (t=29 min), the system quickly reverts (<5 min) to its initial state.

The next challenge was to incorporate variable-temperature capabilities into the probe. There are several possible methods for heating the rotor. The first is to use variable-temperature gas. This method is the most common for conventional MAS probes, and is the most developed technologically. It has the advantage in that samples can be either heated or cooled, but has the disadvantage in that another gas stream is introduced into the spinning module which must be isolated from the reactant/product gas stream. Two alternative methods which do not require a heating gas stream are RF heating and laser heating [25]. Both of these methods have been shown to be effective for heating MAS rotors to very high temperatures. They have the disadvantage in that they would require additional technological development before they could be easily implemented (i.e. directing a laser onto the rotor, effective platinum coating for RF heating), nor are they as robust as variable-temperature gas. Also, these methods produced large temperature gradients, whereas variable-temperature heating provides a much more uniform heating of the sample. For this reason, we chose to use a gas stream to heat the rotor, despite the obvious problems that it might introduce by mixing with the reactant/product gas stream. However, if pure N_2 gas is used as both the carrier gas and the variable-temperature gas, mixing of the two gas streams should not complicate the interpretation of either the NMR spectrum or the GC results.

We began testing the variable-temperature capabilities of our probe by using the ^{207}Pb chemical shift of $Pb(NO_3)_2$ to measure the temperature of the sample region. There have been two reports which correlate the ^{207}Pb chemical shift of $Pb(NO_3)_2$ with temperature [25,26]. One report states that the chemical shift changes by 0.775 ppm/°C [25], and the other that it changes by 0.753 ppm/°C [26]. We chose to use 0.764 ppm/°C as an average of the two reported values. Since magic-angle spinning results in a small amount of sample heating even at slow speeds, we allowed the sample to equilibrate at room temperature while spinning before calibrating the temperature. For all of our variable-temperature experiments, we used a constant reproducible gas flow to ensure that temperature measurements were equivalent from experiment to experiment. Typical spinning rates at the beginning of the experiments were between 1.5 and 2.0 kHz, and during the course of the experiment often decreased to 1.1–1.4 kHz. At high temperatures, the measured temperature appeared to be independent of the spinning speed.

Fig. 9 shows the variable-temperature ^{207}Pb MAS NMR spectrum of $Pb(NO_3)_2$ as it was heated in the flow MAS system using variable-temperature gas heated from 30° to 335°C. The spectrum at 30°C

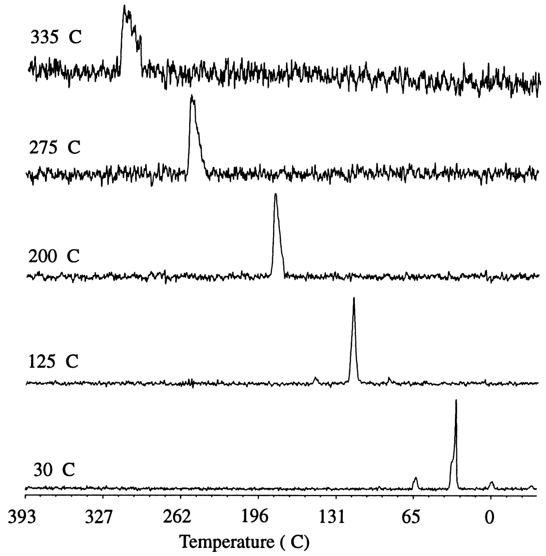

Fig. 9. ^{207}Pb VT MAS NMR of $Pb(NO_3)_2$ at 1.5 kHz spinning rate and various temperatures. Temperature given for each spectrum was the indicated temperature on the Chemagnetics VT controller and the chemical shift scale has been converted to calculated temperature.

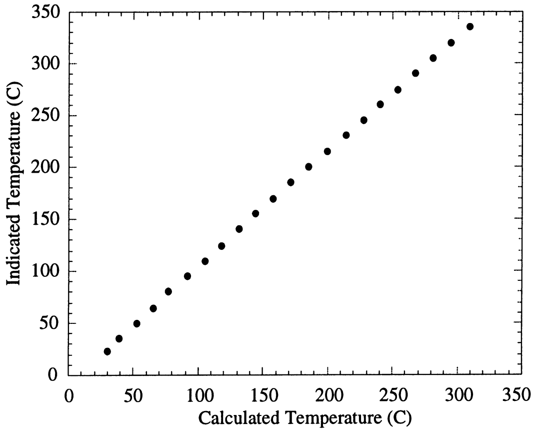

Fig. 10. Temperature calibration of the indicated temperature to that calculated from chemical shift data using a correlation constant of 0.764 ppm/°C for $Pb(NO_3)_2$.

shows an asymmetric line shape because the magic angle was slightly off and could not easily be adjusted in this particular configuration. Spinning sidebands on either side of the isotropic peak indicated that the rotor was spinning at a rate of 1.55 kHz, which was confirmed by the tachometer. As the temperature was increased, the line became successively broader, indicating thermal gradients across the rotor. At the highest temperature of 335°C, the line is ca. 15 ppm broad, indicating a temperature gradient of ca. 20°C. Shown in Fig. 10 is the correlation of the indicated temperature of the variable-temperature gas with the temperature as determined from the chemical shift of the $Pb(NO_3)_2$. The chemical shift values were taken from either the top of the peak at lower temperatures or at the leading edge of the peak at higher temperatures. Remarkably, the data correspond to a straight line, with a correlation constant of 0.9998. The slope of the line, which should be unity, is closer to 1.1. There are several possible explanations why the slope is not equal to unity. First, the equation that we are using to correlate temperature with chemical shift may not be completely correct. If the two proposed values for relating chemical shift to temperature were used, the slope of the lines would vary by 0.03. A more likely explanation for a slope of 1.1 is that the variable-temperature gas is cooled after it exits the variable-temperature stack (where the gas temperature is measured). The gas flow rate is much lower than is used for the conventional MAS systems to avoid putting torque on the rotor while it is spinning. This allows the gas to cool in the variable-temperature gas inlet. It could also be that there is heat loss through the axle of the rotor. It is likely that the slope of the line can be decreased by using a higher variable-temperature gas flow rate and/or providing better insulation between the variable-temperature stack and spinning module. Alternatively, a small amount of $Pb(NO_3)_2$ can be incorporated into the spinning module to serve as an in situ temperature sensor.

We were also interested in considering the effect of flow on temperature. Fig. 11 shows the effect on sample temperature of flowing N_2 gas through the reactant/product gas stream at a rate of 300 ml/min through the rotor with a variable-temperature gas flow temperature of 225°C and a spinning rate of 1.2 kHz. The most noticeable effect is that, with the N_2 gas flow turned on, the line becomes broader and shifted by ca. 4 ppm. This indicates that the entire sample is being slightly cooled, but that there is a temperature gradient caused by part of the sample being cooled more than another part of the sample. This effect is reproducible, since Fig. 12 shows the temperature as determined from the $Pb(NO_3)_2$ chemical shift when the N_2 gas

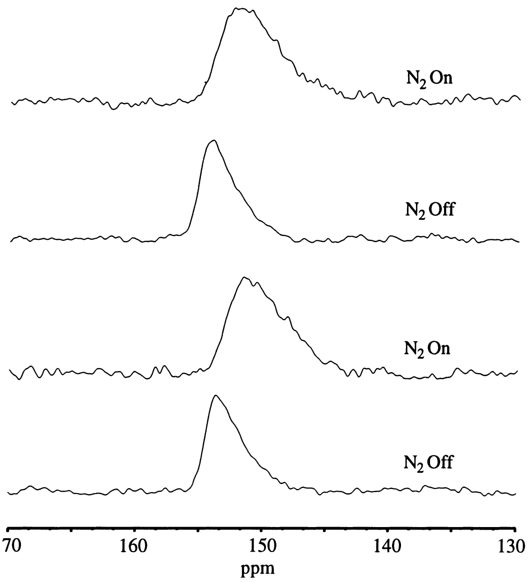

Fig. 11. ^{207}Pb VT MAS NMR spectrum of $Pb(NO_3)_2$ at 1.2 kHz spinning rate and 200°C with, and without, N_2 gas flow at 300 ml/min. The change in chemical shift is caused by the N_2 gas cooling the $Pb(NO_3)_2$.

flow was alternatively turned on and off. There is consistently a 4–5°C temperature change upon changing flow, with a time to reach equilibrium of <3 min. This experiment demonstrates that there will be a slight but significant change in sample temperature with reactant/product gas flowing through the rotor.

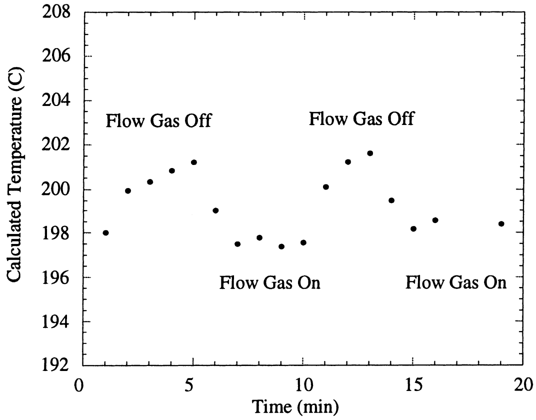

Fig. 12. Plot of sample temperature vs. time as a function of N_2 gas flow.

The ability of the probe to perform catalysis was investigated next. The conversion of methanol-to-gasoline-range hydrocarbons (MTG) on zeolite HZSM-5 has been the subject of intense research for many years, and there have been several NMR studies of this reaction [7,13,15]. It is also an excellent test reaction in that ^{13}C-labeled methanol is readily available and reasonably priced. The first experiment we performed was to place nonactivated zeolite HZSM-5 into a flow-MAS rotor and add a drop of ^{13}C-labeled methanol to the rotor. No flow gas was used during this experiment. Since the rotor was not sealed, any volatile compounds that were not strongly adsorbed to the surface of the catalyst could exit through either the reactant or product end of the rotor. Fig. 13 shows the ^{13}C MAS NMR spectrum of the reactions of methanol on HZSM-5 as it was heated to various temperatures. At room temperature, a peak at 51 ppm due to methanol was easily visible in the NMR spectrum. As the sample was heated to 100°C (all temperatures reported for this experiment correspond

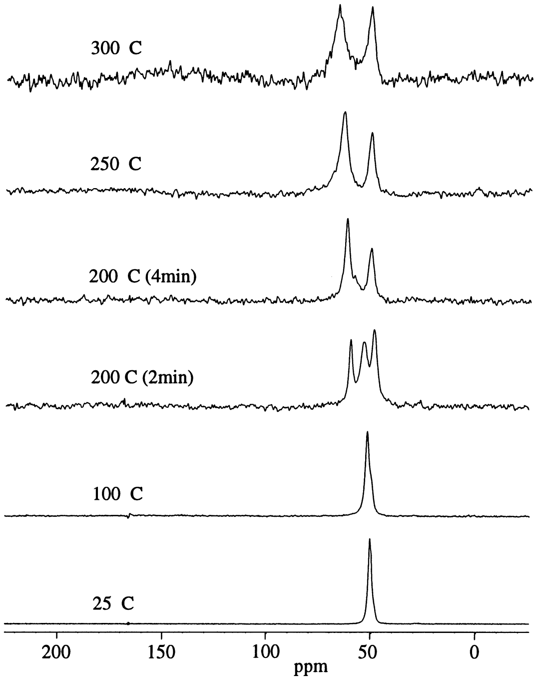

Fig. 13. ^{13}C MAS NMR spectra of ^{13}C-labeled methanol reacting on zeolite HZSM-5 at a 1.4 kHz spinning rate and various temperatures.

to the indicated variable-temperature gas), the chemical shift of the methanol shifted downfield by ~1 ppm and there was a shoulder on the upfield side of the peak. The change in chemical shift with temperature has been observed previously in studies of dimethyl ether reacting on zeolite HZSM-5 [15]. Upon increasing the temperature to 200°C, there are three peaks in the spectrum at 51, 56, and 62 ppm, and the signal-to-noise ratio is much worse. The peak at 51 ppm is possibly due to methanol that is not in the catalyst but rather adsorbed on an inert surface, such as the glass wool used to secure the catalyst in the rotor or even the rotor itself. The peak at 56 ppm is methanol adsorbed in the catalyst that is interacting strongly with a Brønsted acid site. The chemical shift is probably an average of protonated and non-protonated methanol. At high temperatures, the protonated methanol is favored. The peak at 62 ppm indicates the formation of dimethyl ether. It is probable that at this temperature much of the methanol is escaping the zeolite and is exiting through the reactant and product ends of the rotor, which accounts for the reduced signal. After a longer time at 200°C, most of the methanol that is in the catalyst has been converted to dimethyl ether. As the sample is heated to 250°C, and finally to 300°C, the chemical shift of the peak due to dimethyl ether changes from 62 to 67 ppm, whereas the peak due to methanol remains relatively unchanged. The intensity of the dimethyl ether peak is also decreasing, indicating possible desorption and/or conversion to hydrocarbons. The sensitivity was not adequate enough to observe any potential hydrocarbon formation. This experiment shows that it is possible to perform catalytic experiments using the same configuration as would be used in flow experiments.

The next experiment was designed to test the flow capability of the probe at high temperatures. N_2 gas at a rate of 300 ml/min was bubbled through unlabeled methanol and into the flow-MAS probe (spinning at 1.4 kHz), which contained zeolite HZSM-5 and was heated to an indicated gas temperature of 225°C. The product stream was directed into a condenser cooled with a dry ice/acetone bath (−78°C) to collect any products formed during the reaction. Approximately 3–4 ml of methanol was consumed during a one-hour experiment. During the experiment a liquid collected at the bottom of the trap. After the experiment, the trap was removed from the dry ice/acetone bath and warmed to room temperature. During the warming process the liquid evaporated, indicating that it had a boiling point lower than room temperature, and is consistent with dimethyl ether, which is a gas at room temperature (b.p. −25°C) [27].

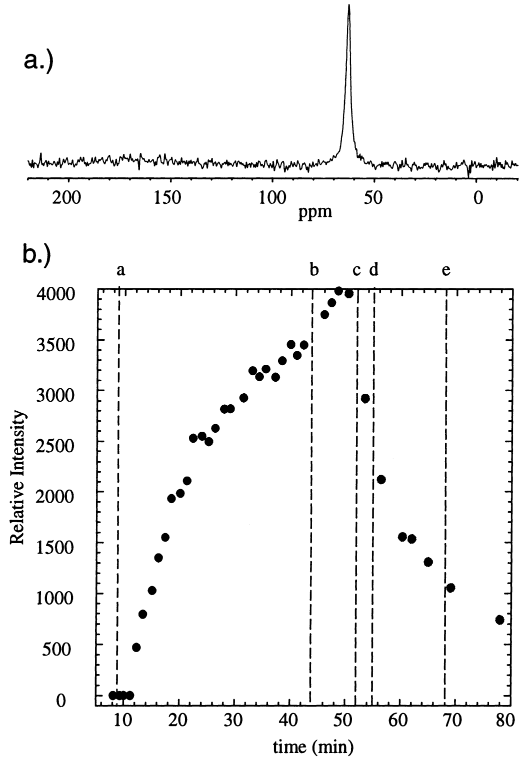

Fig. 14. (a) ^{13}C VT MAS NMR spectrum showing dimethyl ether peak after 50 min of methanol/N_2 (300 ml/min) flow over zeolite HZSM-5 at 1.4 kHz spinning rate and 200°C. (b) (a) Begin flow of ^{13}C-labeled methanol/N_2; (b) methanol bypassed (only N_2 flow); (c) temperature increased to 275°C; (d) temperature increased to 315°C; and (e) N_2 flow gas and heater discontinued.

Fig. 14 shows the results of the same experiment as described above, except that ^{13}C-labeled methanol was used instead of unlabeled methanol, and ^{13}C NMR spectra were acquired during the experiment. All of the spectra acquired were very similar, in that only one peak was observed due to dimethyl ether. No peak for methanol was observed. The peak from dimethyl ether increased during the course of the experiment, indicating an accumulation of dimethyl ether on the catalyst over time. After 34 min, the methanol was bypassed, and only N_2 gas flowed through the rotor. The dimethyl ether peak continued to increase, presumably due to methanol that still remained in the injection line after the bubbler was bypassed. After 42 min the temperature was increased to 275°C, and 3 min later increased to 315°C. The dimethyl ether peak rapidly decreased in intensity, due to either desorption or conversion to hydrocarbon products. The desorption continued to occur for the next 13 min. At that time, both the N_2 flow and heater were turned off. Even under these conditions desorption continued to occur, as the catalyst remained above 250°C for several minutes before cooling.

This successful test of the catalytic capabilities of the probe also raises some questions, especially as to why no peak was observed for methanol. This would seem to indicate that the methanol is immediately converted to dimethyl ether on the catalyst, and suggests that no equilibrium exists between methanol and dimethyl ether in a flow reactor. This is quite different than in a batch reactor, such as a sealed NMR rotor, where methanol and dimethyl ether are observed to be in rapid equilibrium, and the concentration of methanol at 200°C is relatively high [15]. Another explanation for why we do not observe any methanol peak in this experiment is that the flow rates used in these experiments are very high, in that roughly 5 ml of gas passes through the 1 ml sample volume in one second. The residence time of the reactant on the catalyst is $\sim$0.2 s, and the time that the methanol spends in the reactor is much less than that. In future, we will perform experiments with lower flow rates, which should increase our sensitivity by keeping the reactants/products in the reactor for a longer time and will also reduce the amount of reactant used in the experiment.

4. Conclusion

In this paper, we have shown a new design for an isolated flow MAS NMR probe that uses ceramic ball bearings rather than conventional air bearings. We demonstrated that high-resolution CP/MAS NMR spectra could be acquired while spinning with ceramic bearings. We also illustrated the flow aspects of the probe at room temperature by observing the adsorption of methanol on zeolite HZSM-5 and the change in conformation of a vapochromic sensor material when exposed to benzene and hexane. We have also demonstrated the variable-temperature capabilities of the probe by observing the change in chemical shift of $Pb(NO_3)_2$ with temperature, and have shown that the probe can be used to temperatures >300°C. We have also proven the feasibility of this probe design for studying heterogeneous catalysis reactions under flow conditions by studying the conversion of methanol to dimethyl ether on zeolite HZSM-5. Unlike other probe designs, we demonstrated the ability to simultaneously collect products while collecting spectra of the reaction occurring in the NMR rotor. In future, we plan to increase the variable-temperature capabilities to >400°C and improve the reliability of the probe, as well as to apply this technique in studying additional problems in heterogeneous catalysis.

Acknowledgements

This research is funded by the National Science Foundation under grant #CHE-9624161. We would like to thank the University of Minnesota Chemistry machine shop, especially Joel Fischer and Harley Steinbrenner, for assistance in designing and constructing the flow MAS probe.

References

[1] Haw, J.F. in: A.T. Bell, A. Pines (Eds.), NMR Techniques in Catalysis, Marcel Dekker, New York, 1994, pp. 139.
[2] J.F. Haw, J.B. Nicholas, T. Xu, L.W. Beck, D.B. Ferguson, Acc. Chem. Res. 29 (1996) 259.
[3] G.W. Haddix, J.A. Reimer, A.T. Bell, J. Catal. 106 (1987) 111.
[4] M.S. Went, J.A. Reimer, J. Am. Chem. Soc. 114 (1992) 5768.
[5] A. Bendata, G. Chinchen, N. Clayden, B.T. Heation, J.A. Iggo, C.S. Smith, Catal. Today 9 (1991) 129.
[6] M.W. Anderson, J. Klinowski, J. Am. Chem. Soc. 112 (1990) 10.
[7] J. Klinowski, Chem. Rev. 91 (1991) 1459.
[8] M. Pruski, D.K. Sanders, T.S. King, B.C. Gerstein, J. Magn. Reson. 96 (1992) 574.
[9] J.F. Haw, B.R. Richardson, I.S. Oshiro, N.D. Lazo, J.A. Speed, J. Am. Chem. Soc. 111 (1989) 2052.
[10] E.J. Munson, D.B. Ferguson, A.A. Kheir, J.F. Haw, J. Catal. 136 (1992) 504.
[11] E.J. Munson, D.K. Murray, J.F. Haw, J. Catal. 141 (1993) 733.
[12] J.F. Haw, Anal. Chem. 60 (1988) 559A.
[13] E.J. Munson, A.A. Kheir, N.D. Lazo, J.F. Haw, J. Phys. Chem. 96 (1992) 7740.

[14] E.J. Munson, A.A. Kheir, J.F. Haw, J. Phys. Chem. 97 (1993) 7321.
[15] F.G. Oliver, E.J. Munson, J.F. Haw, J. Phys. Chem. 96 (1992) 8106.
[16] M. Hunger, T. Horvath, J. Chem. Soc., Chem. Commun., 1423 (1995).
[17] M. Hunger, T. Horvath, J. Catal. 167 (1997) 187.
[18] P. Goguen, J.F. Haw, J. Catal. 161 (1996) 870.
[19] E. MacNamara, D. Raftery, J. Catal. 175 (1998) 135.
[20] G.E. Maciel, 215th National Meeting of the American Chemical Society, Dallas, TX, March 29–April 3, 1998.
[21] A.D. Bax, N.M. Szeverenyi, G.E. Maciel, J. Magn. Reson. 52 (1983) 147.
[22] H.Y. Carr, E.M. Purcell, Phys. Rev. 94 (1954) 630.
[23] S. Meiboom, D. Gill, Rev. Sci. Instr. 29 (1958) 688.
[24] C.A. Daws, C.L. Exstrom, J.R. Sowa, K.R. Mann, Chem. Mater. 9 (1997) 363.
[25] D.B. Ferguson, J.F. Haw, Anal. Chem. 67 (1993) 3342.
[26] A. Bielecki, D.P. Burum, J. Magn. Reson. 116 (1995) 215.
[27] David R. Lide (Ed.), CRC Handbook of Chemistry and Physics, 72nd edn., CRC Press, Ann Arbor, 1992, pp. 3–322.